

Preparation and characterization of polylactide/poly(ϵ -caprolactone)-poly(ethylene glycol)-poly(ϵ -caprolactone) hybrid fibers for potential application in bone tissue engineering

YueLong Wang^{1,2,*}
Gang Guo^{1,*}
HaiFeng Chen²
Xiang Gao¹
RangRang Fan¹
DongMei Zhang¹
LiangXue Zhou²

¹State Key Laboratory of Biotherapy and Cancer Center, ²Department of Neurosurgery, West China Hospital, West China Medical School, Sichuan University, Chengdu, People's Republic of China

*These authors contributed equally to this paper

Abstract: The aim of this study was to develop a kind of osteogenic biodegradable composite graft consisting of human placenta-derived mesenchymal stem cell (hPMSC) material for site-specific repair of bone defects and attenuation of clinical symptoms. The novel nano- to micro-structured biodegradable hybrid fibers were prepared by electrospinning. The characteristics of the hybrid membranes were investigated by a range of methods, including Fourier transform infrared spectroscopy, X-ray diffraction, and differential scanning calorimetry. Morphological study with scanning electron microscopy showed that the average fiber diameter and the number of nanoscale pores on each individual fiber surface decreased with increasing concentration of poly(ϵ -caprolactone)-poly(ethylene glycol)-poly(ϵ -caprolactone) (PCEC). The prepared polylactide (PLA)/PCEC fibrous membranes favored hPMSC attachment and proliferation by providing an interconnected, porous, three-dimensional mimicked extracellular environment. What is more, hPMSCs cultured on the electrospun hybrid PLA/PCEC fibrous scaffolds could be effectively differentiated into bone-associated cells by positive alizarin red staining. Given the good cellular response and excellent osteogenic potential in vitro, the electrospun PLA/PCEC fibrous scaffolds could be one of the most promising candidates for bone tissue engineering.

Keywords: electrospinning, PLA, PCEC, hPMSCs, bone tissue engineering

Introduction

Critical-size bone defects remain a major health care issue due to the difficulties in reconstructing large bone segments, and are caused by various diseases, such as trauma, abnormalities, congenital deficiency, or carcinological resection.^{1,2} The recent gold standard for treatment remains bone grafting with autologous or allogeneic bone graft. The number of bone graft procedures in the US has been estimated to be over 1.5 million every year, making bone second only to blood on the list of transplanted materials.³ Available quantities are limited, however, and the harvesting procedure is burdened by comorbidities.^{4,5} With an increasing demand for and decreasing supply of traditional bone graft tissue, tissue engineering techniques are being developed and applied in clinical use as alternatives.⁶⁻⁹ Recently, combined cells with fibrous scaffolds have been shown to be an effective way to treat bone defects and promote bone regeneration.^{10,11}

The extracellular matrix (ECM) is a complex interconnected nano- and micro-ranged fibrous network, which could regulate various cellular functions such as adhesion, migration, proliferation, differentiation, and tissue morphogenesis.¹² As such, the

Correspondence: Gang Guo;
LiangXue Zhou
West China Hospital, West China
Medical School, Sichuan University,
Three People in South Section of No. 17,
Chengdu, People's Republic of China
Tel +86 28 8516 4063
Fax +86 28 8516 4060
Email guogang@scu.edu.cn;
zhxlxl@163.com

natural ECM is a multifunctional nanocomposite that has motivated researchers to design synthetic ECM substitutes. A number of different materials and methods have been used for developing scaffolds for ECM mimicking, with nano- or microfiber scaffolds used frequently.¹² A variety of techniques have been developed for polymer nano- or microfiber fabrication in recent years, which include electrospinning, drawing, template synthesis, phase separation, and self-assembly.^{13–15} Electrospinning technology is a simple method by which to generate nonwoven fibrous articles, with fiber diameters ranging from tens of nanometers to microns.^{8,16,17} This method of scaffold fabrication has gained importance in many specific targets, such as tissue engineering,^{1,18} wound dressing,¹⁹ and drug delivery systems.²⁰ The high surface-to-volume ratio of the scaffolds, which created by ultrafine and continuous micron to nanofiber structures, contributes significantly to improve the level of protein adsorption and subsequent cell attachment. In selecting different parameters, it is desirable to control not only the fiber diameter, but also the internal morphology.²¹ Nanoporous fibers are of interest for applications such as filtration or the preparation of functional tissue engineering substitutes by fiber templates.²²

In general, a candidate of biodegradable and biocompatible polymer for biomaterials should possess appropriately mechanical properties, which are suitable for target applications and guarantee inherent nontoxicity.²³ In recent years, hydrolysable and biocompatible copolymers of polylactide (PLA),²⁴ poly(glycolic acid),²⁵ poly(ϵ -caprolactone) (PCL),¹⁹ poly(lactide-co-glycolide),²⁰ poly(vinyl alcohol),²⁶ and poly(butylene succinate)²⁷ have been used for biomedical scaffolds. They have been gradually approved by the US Food and Drug Administration for internal use in the human body. PLA is one of the most widely used biocompatible and biodegradable biomedical materials.¹⁸ However, due to its strong hydrophobicity, inherent brittle nature and low heat distortion temperature. PLA has been restricted its further applications in tissue engineering.^{18,28} As such, different strategies have been developed to improve PLA. Some reports in the literature have stated that improvement of the properties is attributed to microphase structure difference generated as a result of formation of many stereocomplex crystallites, which acted as intermolecular crosslinks.^{28,29} The physical method of modifying the properties is to blend the PLA with different kinds of polymers and/or other fillers of complementary property features, such as hydroxyapatite,¹⁸ PCL,^{30,31} poly(butylene succinate)³² and poly(ethylene glycol) (PEG).³³ Recently, a paper reported that ABA triblock copolymer of poly(D-lactide)-mid-block-poly(D-lactide) was used as a toughening agent for PLA through a blending

method.²⁸ These PLA/triblock copolymer blends form a morphology that can be described as stereocomplex crystallites serving as nanoreinforcements dispersed in a continuous amorphous phase matrix. In our laboratory, we obtained an amphiphilic triblock copolymer, Poly(ϵ -caprolactone)-poly(ethylene glycol)-poly(ϵ -caprolactone) (PCL-PEG-PCL, PCEC) by incorporating PEG into the PCL main chain.²⁰ Earlier literature has reported that PCEC exhibited good potential in forming cell scaffold complexes because of its high biodegradation rate, amphiphilic nature, and biocompatibility.⁸ Here, our hypothesis was that this ABA triblock copolymer could also be used in improving PLA by the blending method.

Mesenchymal stem cells (MSCs), originating from various sources, are capable of differentiating into cells of different lineages under specific permissive conditions.^{3,34–36} MSCs have attracted a great deal of interest because they are one of the potential cell sources for tissue engineering and regenerative medicine, can be transplanted across major histocompatibility complex barriers without the need for immune suppression, and are not subject to the ethical considerations of embryonic stem cells.^{37,38} In order to search for easily accessible sources of multipotent MSCs, various groups have looked into cells from different tissues, including bone marrow, umbilical cord blood, mobilized peripheral blood, and adipose tissues.^{35,37,39} MSCs derived from such tissues have many disadvantages however, including insufficient supply of stem cells, decreased proliferation and differentiation capacity with age, and development of tumors after stem cell transplantation.⁴⁰ Recently, human placenta-derived MSCs (hPMSCs) have been discovered as a new source of stem cells.^{40,41} Obtaining the organ is not an invasive procedure, as the placenta is expelled after the birth of the neonate. Cells of the placenta are fetal. Therefore, preservation of placenta at birth would provide a once-in-a-lifetime opportunity to preserve “young” autologous stem cells.⁴⁰ Literature has shown that hPMSCs could remain viable and reproducible during proliferation *in vitro* and could be differentiated *in vitro* into neuron-like cells (ectoderm), adipocytes, osteo-blasts, endothelial-like cells (mesoderm), and hepatocytes (endoderm) when cultured in specific induction medium.^{8,41–43}

In the present study, novel PLA/PCEC hybrid electrospinning fibrous membranes with a nanoporous surface were obtained, and the chemical and physical properties of the PLA/PCEC hybrid scaffolds were investigated by Fourier transform infrared (FT-IR) spectroscopy, X-ray diffraction (XRD), differential scanning calorimetry (DSC), and scanning electron microscopy (SEM), among other methods.

The aim of this study was to develop this osteogenic biodegradable composite graft consisting of hPMSC material for site-specific repair of bone defects and attenuation of clinical symptoms.

Materials and methods

Materials

Semicrystalline-grade PLA 4032D ($M_w=160,000$) with approximately 2% of D-lactic acid monomer was purchased from NatureWorks LLC (Minnetonka, MN, USA). PEG ($M_n=4,000$), ϵ -caprolactone, and stannous octoate ($\text{Sn}[\text{Oct}]_2$) were supplied by Sigma-Aldrich (St Louis, MO, USA). Dichloromethane (CH_2Cl_2) was purchased from KeLong Chemicals (Chengdu, People's Republic of China). All the chemicals used in this experiment were analytical reagent grade.

Synthesis and characterization of PCEC copolymer

PCEC copolymer was synthesized in our laboratory. Briefly, PCEC copolymer was synthesized by introducing a known amount of ϵ -caprolactone and PEG (weight ratio =8:1) into a dry glass ampoule under N_2 atmosphere, with $\text{Sn}(\text{Oct})_2$ (0.5% w/w of total feed stock) added as catalyst. During reaction, the system was stirred slowly, with the reaction temperature kept at 135°C . After 8 hours, the system was rapidly heated to 180°C under vacuum within 30 minutes. After being cooled to room temperature under N_2 atmosphere, the mixtures were first dissolved in methylene chloride and then precipitated from the filtrate using excess analytical reagent-grade cold petroleum ether.²⁰ Finally, the mixtures were filtered and vacuum-dried to constant weight, and kept in air-tight bags in desiccators before use.

Gel permeation chromatography ([GPC] 1100 series; Agilent, Santa Clara, CA, USA) was used to explore the molecular weights and distribution of PCEC copolymers. PCEC copolymer samples were dissolved in tetrahydrofuran (freshly distilled before use) at a concentration of 1–2 mg/mL. The mobile phase was tetrahydrofuran using a regularity elution at a flow rate of 1.0 mg/mL. The external and column temperatures were kept at 35°C . Proton nuclear magnetic resonance ($^1\text{H-NMR}$) spectra (in CDCl_3) were recorded on a Varian 400 spectrometer (Varian Medical Systems, Palo Alto, CA, USA) at 400 MHz, using tetramethylsilane as internal reference standard.

Preparation of PLA/PCEC nanofiber

Figure 1 illustrates the setup of the electrospinning apparatus, which consisted of a high-voltage power generator

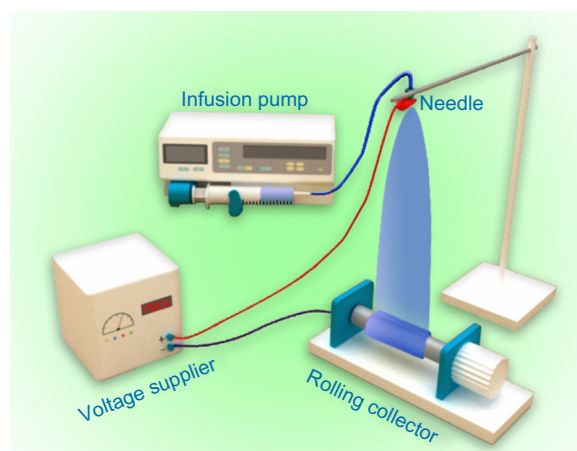


Figure 1 Schematic illustration of the electrospinning apparatus used in this study.

(High Voltage Technology Institute, Beijing, People's Republic of China), an infusion pump (Smith Medical Instrument Company, Zhejiang, People's Republic of China), and a 20 mL plastic syringe (BD, Franklin Lakes, NJ, USA) equipped with a stainless-steel blunt-ended needle with an inner diameter of 0.5 mm. Electrospun PLA/PCEC fibers were deposited onto rolling collector (0.5 m/second) for 60 minutes. A silicone tube was used to connect the syringe and a blunt-end needle, which was set up vertically. The concentration of PLA/PCEC solution was set at 8% (w/v), and PCEC content was 0, 25, 50, 75, and 100 wt%. For each PLA/PCEC suspension, 20 mL was fed into a plastic syringe, which was injected by the syringe pump at a flow rate of 7 mL/hour. The distance between the nozzle and the aluminum foil collector was adjusted to 12 cm. A voltage of 18 kV was applied to generate the PLA/PCEC jet. All experiments were carried out at $20^\circ\text{C}\pm 3^\circ\text{C}$ and the environmental humidity was controlled to between 45% and 60%. The obtained PLA/PCEC membranes were left in a vacuum oven at 35°C for 48 hours to eliminate the solvent residue then kept in a desiccator for further characterization and treatment.

Nanofiber characterization

FT-IR and XRD analysis

Attenuated total reflectance–FT-IR spectra of PLA/PCEC hybrid scaffolds were obtained with a Nicolet 6700 FT-IR machine (Thermo Fisher Scientific, Waltham, MA, USA). The crystallinity of PLA/PCEC composite membrane was analyzed by XRD (X' Per Pro MPD DY 1291; Philips, Eindhoven, Netherlands) with Cu K_α radiation ($\lambda=0.1542$ nm; 40 KV; 40 mA) at a scanning rate of $4^\circ/\text{minute}$ in the 2θ range from 10° to 60° .

Thermal properties

Melting temperature (T_m), crystallization temperature (T_c), and glass transition temperature (T_g) of dried PLA/PCEC hybrid membranes were characterized by DSC (NETZSCH 204; NETZSCH, Selb, Germany). Samples were first heated from 20°C to 180°C under N_2 atmosphere at a heating rate of 20°C/minute, and quenched to -10°C at a rate of 10°C/minute, after all reheated to 190°C at a rate of 10°C/minute. Thermogravimetric analysis (TG) and derivative temperature gravimetry (DTG) test was carried out with a TA Instrument (Q500; TA Instruments, New Castle, DE, USA). All samples were 8–10 mg and heated from 20°C to 600°C in an N_2 atmosphere at a heating rate of 10°C/minute.

SEM

The structural morphology of the electrospun PLA/PCEC hybrid scaffolds was investigated by SEM (JSM-5900LU; JEOL, Tokyo, Japan) and the diameters of the electrospun fibers in the composites were determined from SEM micrographs. The samples were coated with gold using a sputter coater (KYKY SBC-12; KYKY Technology Development Ltd, Beijing, People's Republic of China) in advance.

Water contact angle measurement

Water contact angles of PLA/PCEC hybrid membranes were investigated by drop shape analysis (DAS100; KRÜSS, Hamburg, Germany) at room temperature. A drop of 3 μ L of deionized water was dropped on the surface of fibrous membranes and photographed immediately. The contact angle (θ) was obtained from the height (h) and breadth (b) of the drop according to the following equation:

$$\theta = 2 \arctan \frac{2h}{b} \quad (1)$$

Each scaffold was measured at least three times at different positions and the results were averaged.

Mechanical properties

Mechanical properties, in terms of tensile strength and Young's modulus, of the electrospun PLA/PCEC fibrous mats were measured at room temperature and relative humidity of 60% on a universal mechanical testing instrument (Instron 5567; Instron, Norwood, MA, USA). An Instron static load cell of 100 N was employed for all the tension tests. The speed of tensile testing was 5 mm/minute. All specimens of a rectangular shape with dimensions of 50×5 mm² were cut from the collected membranes with a thickness of 0.3–0.6 mm. The stress

and strain were calculated through the machine-recorded force and displacement based on the initial cross-section area and gauge length, respectively. The Young's modulus was calculated through linear regression analysis of the initial linear portion of the stress–strain curves.

Cell culture examination

Isolation and culture of hPMSCs

hPMSCs were isolated in our laboratory from placentas of healthy donor mothers during routine cesarean section births, with full informed consent. Briefly, placenta tissues were minced into a paste-like consistency and rinsed thoroughly in phosphate-buffered saline (PBS); then the tissue pieces were kept in 50 mL tubes (BD) and digested with 1 mg/mL collagenase II (Sigma-Aldrich) for 2 hours at 37°C in an incubated shaker. The collagenase was inactivated by adding proliferation medium (Dulbecco's Modified Eagle's Medium-low glucose [DMEM-LG] [Life Technologies, Carlsbad, CA, USA] with 10% fetal bovine serum [Life Technologies] and 1% penicillin/streptomycin [Life Technologies]). After centrifugation, the supernatant was discarded and the pellet was resuspended in proliferation medium and filtered through a 100 μ m pore filter. Following this, the filtrate was centrifuged to obtain the hPMSCs, which were resuspended in proliferation medium, and cultured at 37°C under an atmosphere of 5% CO_2 in humidified air. The cells were maintained up to passage 4 and collected by trypsin–ethylenediaminetetraacetic acid treatment.

Fluorescence microscopy observation and cell viability

To investigate cell attachment on the surfaces of PLA/PCEC hybrid membranes, the samples were fixed on the bottom of each well and sterilized using ethylene oxide steam for 24 hours at room temperature. hPMSCs were then seeded onto PLA/PCEC hybrid scaffolds containing 50 wt% PCEC at a density of 5×10^3 /mL and cultured with proliferation medium at 37°C under an atmosphere of 5% CO_2 in humidified air. After incubation for 48 hours, hPMSCs were stained with the fluorescent dyes fluorescein isothiocyanate (FITC) (Sigma-Aldrich) and Dil Life Technologies and then observed by fluorescence microscopy.

The viability of hPMSCs cultured on the PLA/PCEC hybrid scaffolds with different PCEC concentration was determined by 3-(4,5-dimethylthiazol-2-yl)-2,5-diphenyl-2H-tetrazolium-bromide (MTT) assay (Roche Diagnostics, Mannheim, Germany). hPMSCs were cultured on the electrospun fibrous scaffolds, which were fixed on the bottom

of 24-well plates in advance, at 37°C under an atmosphere of 5% CO₂ for 2, 4, and 6 days. Subsequently, 100 μL of 5 mg/mL MTT was added to each well and incubated at 37°C under an atmosphere of 5% CO₂. After 4 hours, supernatant was removed, and 650 μL of dimethyl sulfoxide was added to each well for dissolving the blue formazan crystal, then the solution was transferred to 96-well plates. The absorbance of the contents of each well was measured at 570 nm using an enzyme-linked immunosorbent assay microplate reader (Bio-Rad Laboratories, Hercules, CA, USA).

hPMSC differentiation assay on the PLA/PCEC fibrous scaffolds

Cells were seeded on the hybrid PLA/PCEC scaffolds containing 50 wt% PCEC, which fixed on the bottom of 6-well plates in advance, at a density of 5×10⁵ cells/well and cultured with proliferation medium. Two days after seeding, the proliferation medium was replaced with osteogenic differentiation medium (DMEM-LG containing 10% fetal bovine serum, 1% penicillin/streptomycin, 100 nM dexamethasone, 10 mM β-glycerophosphate, and 50 μg/mL ascorbic acid-2-phosphate). After 2 weeks of culture, specimens were rinsed with PBS twice and fixed in 10% buffered formalin, then were dehydrated in a graded ethanol series (30%, 50%, 70%, 80%, 90%, 95%, and 100%). Subsequently, the samples were rinsed twice with hexamethyldisilazane (Kelong Chemicals, Chengdu, People's Republic of China) for 20 minutes and left to air dry overnight in a desiccator. After vacuum drying and gold coating, the samples were viewed by SEM. For alizarin red staining, the samples were gently washed in PBS and fixed with 10% formalin for 30 minutes and then stained

with alizarin red solution (Sigma-Aldrich) for 30 minutes. Calcium deposits were checked by microscope.

Results

Characterization of PLA/PCEC nanofibrous scaffolds

Synthesis of PCEC copolymer

Biodegradable PCEC copolymer was prepared by ring-opening polymerization of ε-caprolactone (ε-CL) initiated by PEG-diol (HO-PEG-OH). Figure 2A shows the synthesis scheme of copolymer PCEC. GPC results (Figure 2B) show that M_n and M_w of PCEC were 2.24×10⁴ and 4.61×10⁴, respectively. Only one single peak existed, which indicated the mono-distribution of macromolecular weight and the absence of any homopolymer of ε-CL or PEG, and also implied that no transesterification or backbiting reactions occurred during polymerization.

FT-IR and ¹H-NMR analysis

Figure 3A shows the FT-IR spectra of pure PLA fiber (Figure 3Ae), PLA/PCEC hybrid fiber (50 wt% PCEC) (Figure 3Ac), and pure PCEC fiber (Figure 3Aa). In the spectrum of the pure PCEC copolymer, the strong peaks at 1180 and 1240 cm⁻¹ were assigned to the characteristic of C–O–C stretching vibrations of repeated –OCH₂CH₂ units of PEG block and the –COO– band stretching vibrations, respectively. The characteristic band at 1,727 cm⁻¹ corresponded to –C=O stretching vibrations of the ester carbonyl group. Two weak peaks at 2,870 cm⁻¹ and 2,940 cm⁻¹ represented vibration of carbon hydrogen (–CH₂–) in PCL block main-chain, which also can be seen in Figure 2Ac.

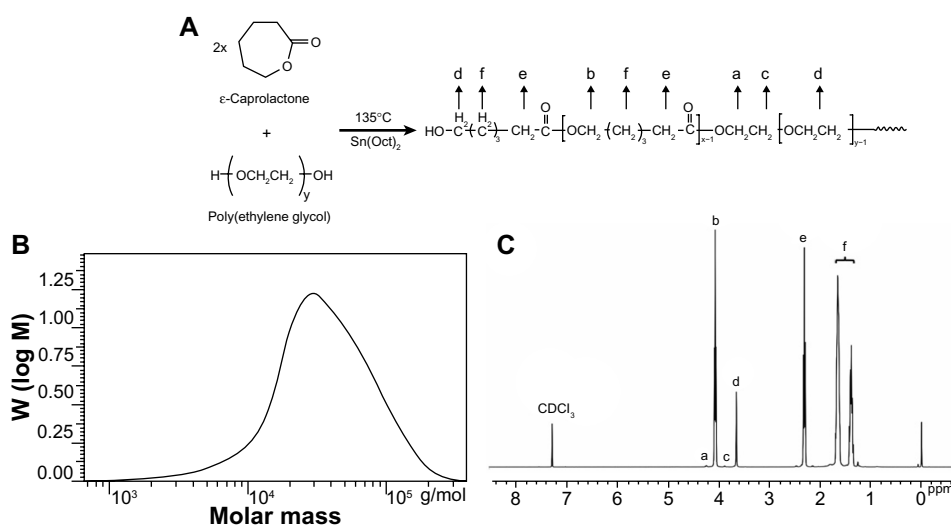


Figure 2 Synthesis scheme (A), gel permeation chromatography curve (B), and proton nuclear magnetic resonance spectra (C) of poly(ε-caprolactone)-poly(ethylene glycol)-poly(ε-caprolactone) copolymer.

Note: M, molecular weight, PPM, parts per million.

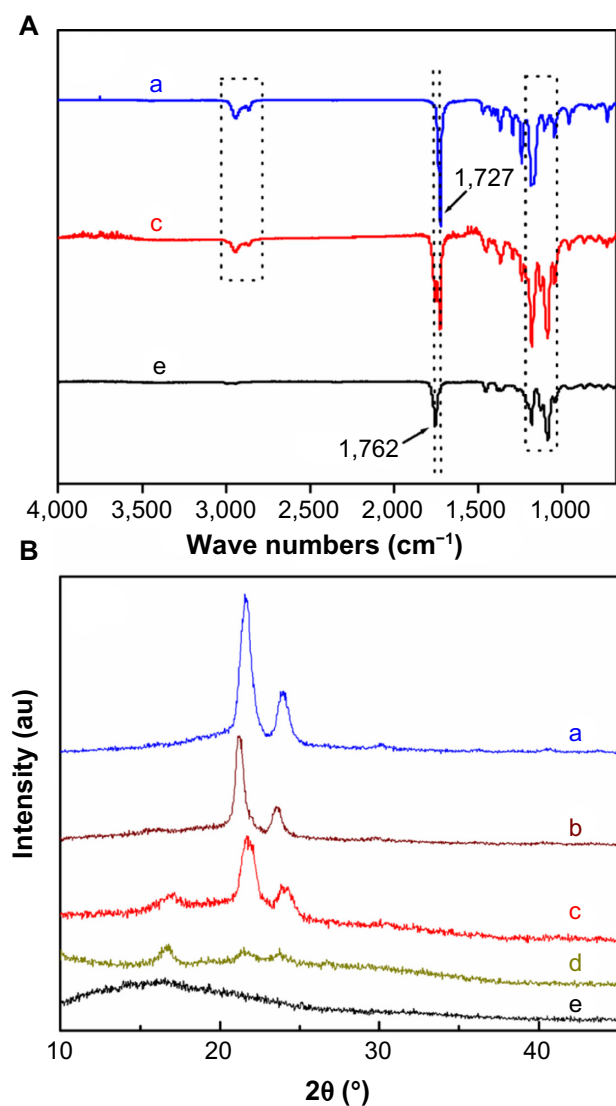


Figure 3 Fourier transform infrared spectra (A) and X-ray diffraction (B) patterns of polylactide/poly(ϵ -caprolactone)-poly(ethylene glycol)-poly(ϵ -caprolactone) (PCEC) nanofibrous membrane with 100 wt% (a), 75 wt% (b), 50 wt% (c), 25 wt% (d), and 0 wt% (e) PCEC concentrations.

In Figure 3Ae, the peaks at 1,762 cm⁻¹ belonged to ester carbonyl $\text{C}=\text{O}$. The main characteristic bands of PLA and PCEC copolymer could be seen in the hybrid membranes.

A typical ¹H-NMR spectrum of PCEC copolymer as well as the detailed assignment of the different peaks is shown in Figure 2C. Peaks at approximately 1.40 ppm, 1.65 ppm, 2.30 ppm, and 4.06 ppm were assigned methylene protons of $\text{-(CH}_2\text{)}_3\text{-}$, $\text{-OCCH}_2\text{-}$, and $\text{-CH}_2\text{OOC-}$ in PCL blocks, respectively. The spectrum shows that two weak peaks, “a” and “c,” were attributed to methylene proton of PEG end units, while peak “d” was attributed to methylene protons of PEG oxyethylene units, and x and y were, respectively, the corresponding block number of PCL and PEG in PCEC copolymers, as shown in Figure 2A. The actual weight ratio

of PCL/PEG of PCEC copolymers was 6.2:1, calculated from ¹H-NMR spectra according to Equations 2–4:

$$\frac{4(y-2)+4}{I_d} = \frac{4}{I_a} \quad (2)$$

$$\frac{2(2[x-1])}{I_b} = \frac{4}{I_a} \quad (3)$$

$$M_{n(\text{PCEC})} = M_{n(\text{PCL})} + M_{n(\text{PEG})} = 2(114x) + 44y \quad (4)$$

where I_a , I_b , and I_d were integral intensities of methylene protons of $\text{-O-CH}_2\text{-}$ in PEG end unit at 4.23 ppm, methylene protons of $\text{-CH}_2\text{OOC-}$ in PCL units at 4.06 ppm, and methylene hydrogen of homosequences of PEG oxyethylene units at 3.65 ppm, respectively.

XRD characterization

XRD profiles of PLA/PCEC hybrid membranes are shown in Figure 3B. From the pure PLA pattern, there was only broad diffusion scattering, which indicated that the pure PLA electrospun nanofibers were non-crystalline. From the pure PCEC pattern, two strong diffraction peaks at 21.5° and 23.8° were the crystalline peaks of PCEC copolymer matrix. From Figure 3Bb–d, two characteristic diffraction peaks could be found at around 21.5° and 23.5°; however, these were slightly weaker than the peaks of pure PCEC. A new peak around 17° appeared when PLA/PCEC hybrid scaffolds contained 25 (Figure 3Bd) and 50 (Figure 3Bc) wt% PCEC.

Thermal behavior

The DSC traces of all samples are shown in Figure 4A and B, and the values of T_m , T_c , and T_g are listed in Table 1. For PLA alone, T_g was observed at around 60°C, and melting temperature was at about 166°C. For pure PCEC and PLA/PCEC hybrid membranes, T_g could not be observed by DSC, although two sharp melting peaks could be seen at 56.8°C–57.1°C and 166.5°C–167.4°C. Figure 5 presents the TG and DTG curves of PLA/PCEC composite, and the temperature at which 5 and 95% weight loss is listed in Table 1. The results revealed that the thermal stability of the PLA/PCEC hybrid membranes containing 25, 50, and 75 wt% PCEC could be divided into two stages while the temperature corresponding to 5 wt% decomposition increased from 204.9°C to 274.8°C with increasing PCEC concentration.

Morphological characterization

The morphology and the fibrous diameter distribution of electrospinning scaffolds were examined by SEM;

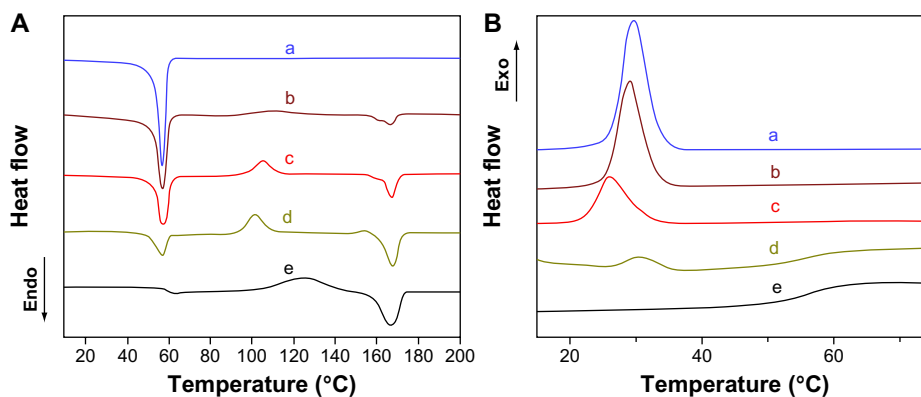


Figure 4 Differential scanning calorimetry curves of poly(lactide)/poly(ϵ -caprolactone)-poly(ethylene glycol)-poly(ϵ -caprolactone) (PCEC) hybrid fibrous scaffolds with 100 wt% (a), 75 wt% (b), 50 wt% (c), 25 wt% (d), and 0 wt% (e) PCEC concentrations.

Notes: (A) Heating process. (B) Cooling process.

Abbreviations: Endo, endothermal; Exo, exothermic.

these results are presented in Figure 6. For pure PLA, the polymer solution could be electrospun into fibers, but the diameter of fibers showed extensive distribution, ranging from 400 nm to 6 μm , and the average size was about $2.2 \pm 1.46 \mu\text{m}$. Some fibers had a spindle-shaped structure, indicating that the electrospinning process was not very smooth, and each individual fiber surface had various nanoscale pores with diameters ranging from 70–300 nm. When PCEC contents were added to 25 wt% and 50 wt%, the composite could be electrospun into continuous fibers and the diameters did not vary so greatly, with the number of nanoscale pores on each individual fiber surface decreased. When PCEC content was increased to 75 wt% however, the diameter of each fiber decreased to $0.85 \pm 0.67 \mu\text{m}$, while numerous beaded structures appeared again. Moreover, for pure PCEC, the diameter of each individual fiber was $1.6 \pm 0.51 \mu\text{m}$, with each appearing to have a smooth and uniform surface.

Water contact angle

The results of water contact angle measurements for the PLA/PCEC hybrid fibrous membranes are shown in Figure 7.

Table I Melting temperature (T_m), crystallization temperature (T_c), glass transition temperature (T_g), and temperature at which 5% ($T_{d,5\%}$) and 95% ($T_{d,95\%}$) weight was loss of poly(lactide)/poly(ϵ -caprolactone)-poly(ethylene glycol)-poly(ϵ -caprolactone) (PCEC) hybrid electrospun nanofibers containing 0, 25, 50, 75, and 100 wt% PCEC

PCEC (wt%)	T_m ($^{\circ}\text{C}$)		T_c ($^{\circ}\text{C}$)	T_g ($^{\circ}\text{C}$)	$T_{d,5\%}$ ($^{\circ}\text{C}$)	$T_{d,95\%}$ ($^{\circ}\text{C}$)
	Peak 1	Peak 2				
0	–	166.0	–	60.7	204.9	362.4
25	56.8	167.4	30.5	65	219.7	362.2
50	57.4	167.4	26.2	–	249.8	389.8
75	57.1	166.5	29.0	–	249.2	374.9
100	56.8	–	29.5	–	274.8	324.3

It can be seen that contact angle values of the PLA/PCEC hybrid membranes were lower than those of pure PLA membrane, and that the values decreased from 126° to 93° with increasing PCEC.

Mechanical characterization

Mechanical behaviors of the electrospun PLA/PCEC hybrid membranes containing 0, 25, 50, 75, and 100 wt% PCEC were measured by tensile test. The representative strain–stress curves are shown in Figure 8, and the obtained data are listed in Table 2. It could be seen that the sample containing 50 wt% PCEC had the largest tensile strength, at $1.59 \pm 0.27 \text{ MPa}$, while the sample containing 75 wt% showed the lowest tensile strength, at $0.20 \pm 0.03 \text{ MPa}$. Meanwhile, the tensile modules of all samples showed the same variation tendency as tensile strength: the sample containing 50 wt% PCEC had the highest value, at $77.7 \pm 4.3 \text{ MPa}$, and the hybrid membrane containing 75 wt% PCEC had the lowest value, at $1.2 \pm 0.2 \text{ MPa}$.

Cell behavior on nanofibrous scaffolds

Cells adhesion and MTT assay

To test the usefulness of PLA/PCEC membranes as a porous scaffold to support cell growth, the hPMSCs were cultured on the PLA/PCEC membranes. After culture for 48 hours, the cell morphology was observed by fluorescence micrographs. As shown in Figure 9B and C, hPMSCs could attach and grow well on the scaffolds after 2 days of culture.

hPMSC proliferation on the five hybrid scaffolds were analyzed by MTT assay at days 2, 4, and 6 after seeding. As shown in Figure 9D, hPMSCs proliferated well on all the substrates compared with control. After 4 and 6 days of culture, hPMSCs seeded on PLA/PCEC hybrid membranes with 0, 25, and 50 wt% PCEC showed almost the same absorbance

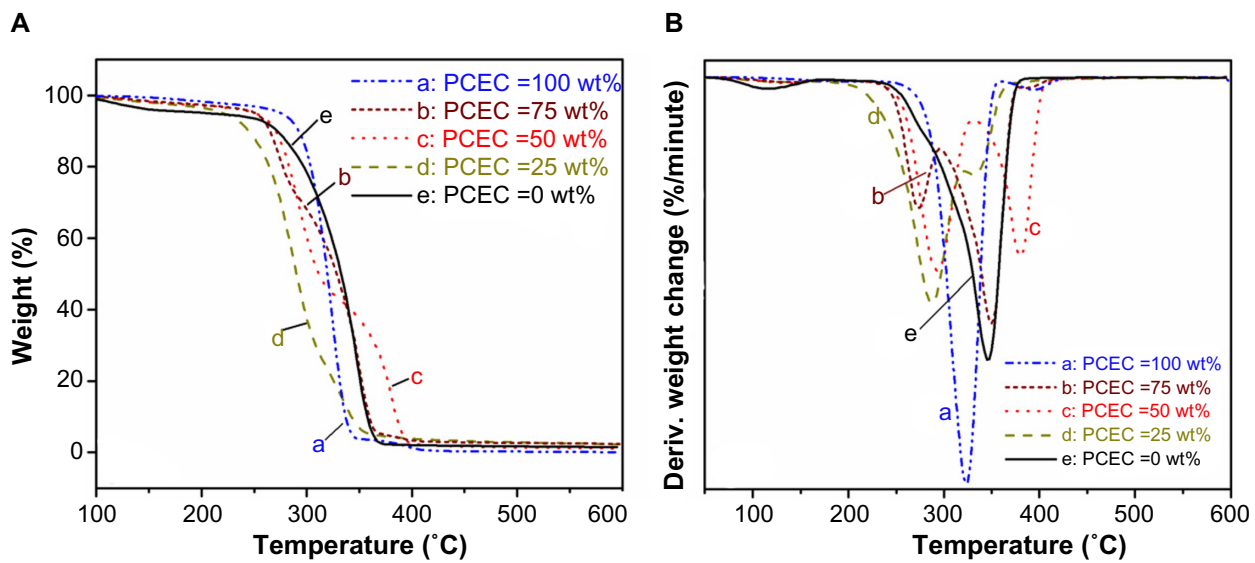


Figure 5 TG (A) and DTG (B) curves of poly(lactide)/poly(ϵ -caprolactone)-poly(ethylene glycol)-poly(ϵ -caprolactone) (PCEC) composite membranes with different PCEC concentrations.

Abbreviations: TG, thermogravimetric analysis; DTG, derivative temperature gravimetry.

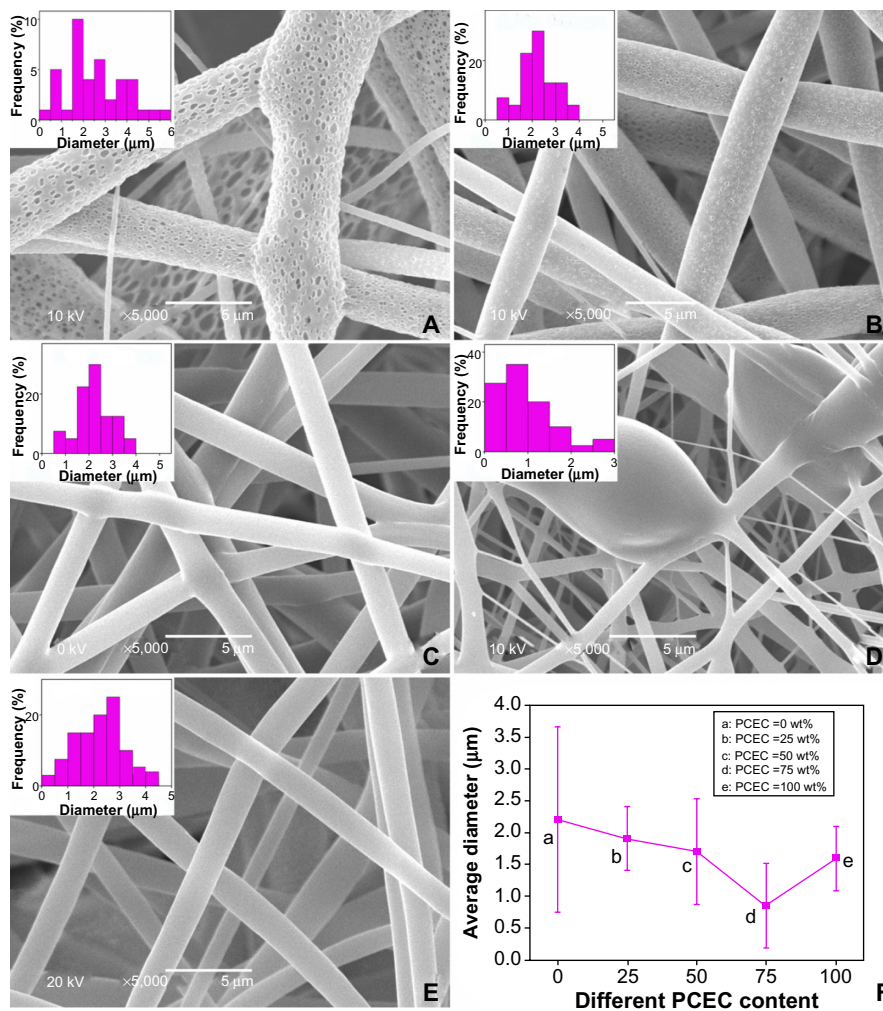


Figure 6 Scanning electron microscope photographs and the diameter distribution of the poly(lactide)/poly(ϵ -caprolactone)-poly(ethylene glycol)-poly(ϵ -caprolactone) (PCEC) hybrid fibers containing (A) 0, (B) 25, (C) 50, (D) 75, and (E) 100 wt% of PCEC.

Note: (F) shows the decreasing of each fiber's diameter with increasing PCEC concentration.

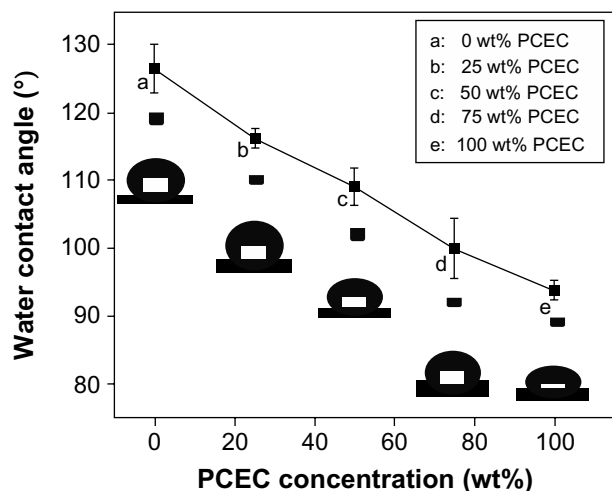


Figure 7 Water contact angle of the polylactide/poly(ϵ -caprolactone)-poly(ethylene glycol)-poly(ϵ -caprolactone) (PCEC) hybrid membranes with different PCEC concentrations.

values compared with control; however, samples containing 75 and 100 wt% PCEC still showed higher absorbance values than control. It should be noted that cell counts after 6 days' incubation had not dramatically increased compared with those of 4 days' incubation.

Differentiation of hPMSCs into osteogenic cells on nanofibrous scaffolds

To investigate the osteogenic differentiation of hPMSCs on PLA/PCEC membranes, alizarin red staining was used to qualitatively confirm calcium deposition, and SEM was used to investigate the morphology of hPMSCs after 2 weeks' incubation with osteogenic differentiation medium. Through SEM imaging and alizarin red staining, it could be

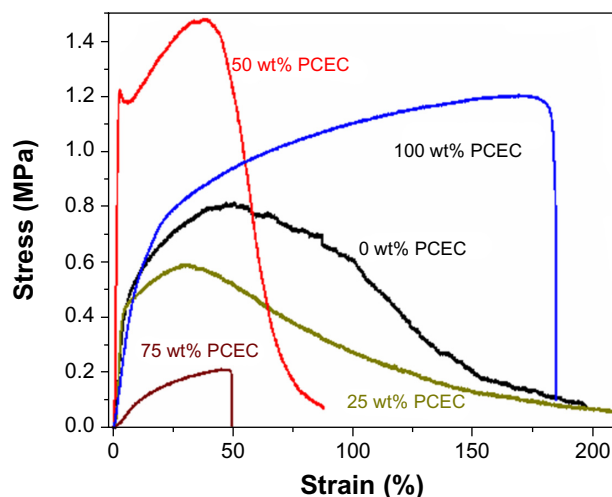


Figure 8 Strain–stress curves of electrospun polylactide/poly(ϵ -caprolactone)-poly(ethylene glycol)-poly(ϵ -caprolactone) (PCEC) fibrous membranes with different PCEC concentrations (0, 25, 50, 75, and 100 wt%).

Table 2 Tensile strength, elongation rate, and Young's modulus of the polylactide/poly(ϵ -caprolactone)-poly(ethylene glycol)-poly(ϵ -caprolactone) (PCEC) hybrid electrospun nanofibers with different concentrations of PCEC

PCEC (wt%)	Maximum tensile strength (MPa)	Elongation at break (%)	Young's modulus (MPa)
0	0.87±0.18	182.3±31.8	14.0±4.2
25	0.59±0.12	206.4±9.8	13.4±3.4
50	1.59±0.27	87.9±9.1	77.7±4.3
75	0.20±0.03	46.3±5.8	1.2±0.2
100	1.23±0.12	183.2±9.1	6.5±0.6

seen that human hPMSCs attached and spread well on the electrospun hybrid PLA/PCEC fibrous scaffolds (Figure 10A) and could be effectively differentiated into bone-associated cells (Figure 10B).

Discussion

The placenta is believed to be a large reservoir of MSCs for therapeutic-scale manufacture. Stem cell lines obtained from the chorion of human placenta have been found to be similar to other MSCs,^{8,40-41} such as bone marrow MSCs and adipose MSCs, which could remain viable and reproducible in vitro, could express markers of pluripotent stem cells (NANOG, OCT-4, SSA-3, etc) and surface markers of mesenchymal cells (CD73, CD90, CD105, etc), and could be differentiated in vitro into osteoblasts, adipocytes (mesoderm), neuron-like cells (ectoderm), and hepatocytes (endoderm) with culturing in differential media.^{1,41} Nazarov et al reported that human chorionic mesenchymal stem cell could remain viable and reproducible for more than 100 doublings (55 passages), which is better than other MSCs.⁴¹ In this study, we successfully prepared PLA/PCEC hybrid membranes by electrostatic spinning technique, and hPMSCs cultured on PLA/PCEC nanofibers showed good cell attachment and robust proliferation and could be induced into osteoblasts when treated with osteogenic differential media, as per a previous study.⁸

The design and fabrication of scaffolds are essential tasks for a functional vital engineered tissue.^{1,7,18} Electrospinning has been proven to be an effective method of fabricating a provisional biomimetic scaffold composed of nano- to microscale fibrous meshes.^{12,16-17} Due to the biomimetic ECMs of a nanofiber scaffold, it might have significant effects on cell behavior.^{2,10,18,19} In addition to the topographical features of a scaffold, the mechanical properties of a scaffold are also an important aspect, which could be regulated by the design of the structure and the material itself. A designed scaffold should not only provide a surface for cell prolifer-

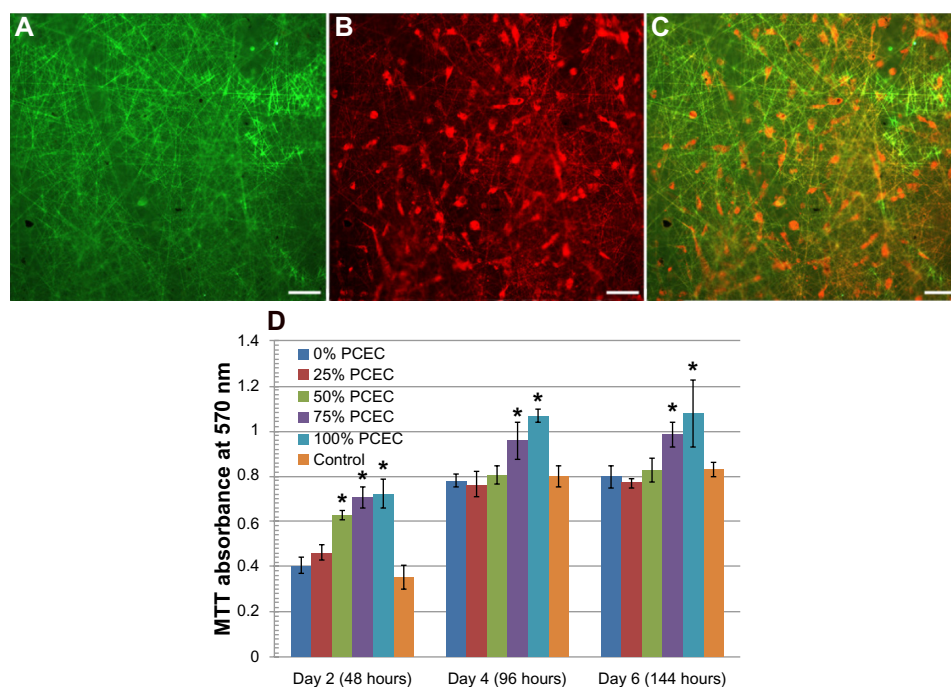


Figure 9 Fluorescence micrographs of PLA/PCEC scaffolds and hPMSCs cultured on PLA/PCEC scaffolds (A-C); MTT assays for proliferation of hPMSCs combined with PLA/PCEC composite membranes (D).

Notes: (A) Green fluorescence images of FITC-stained PLA/PCEC scaffolds. (B) Red fluorescence images of Dil stained hPMSCs cultured on PLA/PCEC scaffolds. (C) Composite of (A and B). Scale bars represent 200 μm . (D) MTT assays for proliferation of hPMSCs combined with PLA/PCEC hybrid nanofibers with different PCEC concentrations cultured for 2, 4, and 6 days. Significance was assessed compared to the control for each time point assayed by one-way analysis of variance. Quantitative data are represented as mean \pm SD, $n=9$. P -values less than 0.05 were considered significant (* $P<0.05$).

Abbreviations: FITC, fluorescein isothiocyanate; MTT, 3-(4,5-dimethylthiazol-2-yl)-2,5-diphenyl-2H-tetrazolium-bromide; PCEC, poly(ϵ -caprolactone)-poly(ethylene glycol)-poly(ϵ -caprolactone); PLA, polylactide; hPMSC, human placenta-derived mesenchymal stem cell; SD, standard deviation.

eration but also maintain sufficient biomechanical support during tissue regeneration and structure degradation. This article presents a novel strategy for bone tissue engineering by culturing hPMSCs on PLA electrospun nanofibers modified by ABA triblock copolymer PCEC.

Biodegradable PCEC triblock copolymers were synthesized by ring-opening copolymerization of PCL initiated by PEG using stannous octoate as catalyst. The $^1\text{H-NMR}$ and GPC results indicate that the PCEC block copolymers were prepared successfully, with a controlled macromolecular weight (Figure 2B and C). The results presented in Figure 3A

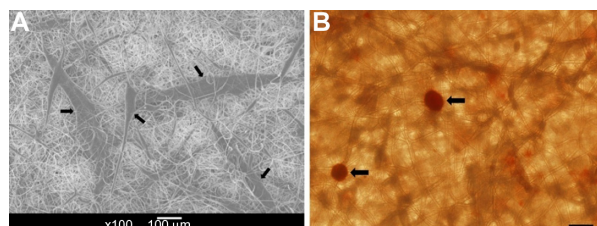


Figure 10 Human placenta-derived mesenchymal stem cells (black arrow), seeded on poly(lactide)/poly(ϵ -caprolactone)-poly(ethylene glycol)-poly(ϵ -caprolactone) nanofibers and treated with osteogenic differentiation medium, observed by scanning electron microscopy (A) and showing positive staining to alizarin red (B) after 2 weeks of culture.

Note: Scale bars represent 100 μm .

reveal that PCEC copolymer exhibited characteristic bands of both PCL and PEG segments, which confirmed the formation of PCEC copolymer. PLA/PCEC hybrid scaffolds exhibited characteristic bands of PLA and PCEC that indicated that the two polymers were blended together when dissolve in dichloromethane together. In Figure 3B, PLA is seen to be a type of semi-crystalline polyester polymer; however, in the process of forming the pattern of pure PLA membrane, no characteristic diffraction peaks occurred, which confirmed that the polymer matrix kept an amorphous structure, while the pattern of pure PCEC membrane revealed that PCEC had a crystalline pattern. Moreover, in the pattern of hybrid membranes (Figure 3Bc and d), peaks at 17.1° and 16.7° could be detected, which indicate that the PLA of PLA/PCEC hybrid membranes were no longer in an amorphous state, but converted into crystalline material.

As seen in Figure 4 and Table 1, the two melting temperatures of PLA/PCEC fibrous scaffolds were higher than those of pure PCEC. The reason might be that interactions between PLA and PCEC after incorporation of PCEC into PLA polymer when electrospun into fibers; however, the sample containing 25 wt% PCEC had a higher crystallization temperature, at 30.5°C , probably because of the homogeneous nucleation

effect of PCEC on the cold crystallization of PLA matrix. From the thermogravimetric analysis (Figure 5 and Table 1), the temperature at which 5% decomposition increase might have been because of the increasing of crystallinity when PCEC concentration was increased. All of those results have proved that thermal stability of PLA/PCEC hybrid membrane was better than that of pure PLA and pure PCEC membrane.

Morphology of the scaffolds was examined by SEM, and images are presented in Figure 6. For pure PLA, there were some spindle-shaped structures among the fibers, and the electrospinning process was not very smooth. This might be due to the intrinsic properties of PLA solution, such as surface tension and viscosity.⁴⁴ Interestingly, the electrospun fiber surface of PLA exhibited nanoscale pores, as also reported by Bognitzki et al, who rationalized that the rapid phase separation induced by the evaporation of the solvent and the subsequent rapid solidification during electrospinning might have accounted for this surface structure.²² With increasing PCEC concentration, the process of electrospinning became smooth, with no spindle-shaped structures formed. We suspected that the low molecular weight (compared with the PLA) might affect the intrinsic properties of the hybrid solution, and PCEC might play the role of lubricant in the mixed solutions, which could reduce the solution viscosity. However, PLA/PCEC with 75 wt% concentration of PCEC could not turn into homogeneous fiber, and numerous beaded structures formed through electrospinning. We speculated that phase separation might be the main reason, which led to formation of amorphous PLA-rich and PCEC-rich phases. The water contact angle of PLA/PCEC hybrid scaffolds was found to gradually decrease from 126.5° to 93.9° with increasing PCEC concentration (Figure 7), which might have been due to the increasing number of hydrophilic phases of PEG and good distribution of fibers.

Mechanical properties, as importance factor of three-dimensional nanoporous scaffolds, were investigated in this study. Based on the results (Figure 8 and Table 2), the sample containing 25 wt% PCEC showed the highest elongation rate at break, while the sample containing 50 wt% PCEC displayed highest tensile strength of all the samples. The results of tensile testing demonstrated that PCEC concentration had a great effect on mechanical properties of the samples. Some reports in the literature have reported that ABA triblock copolymer, such as PCEC used in this study, could modify the mechanical properties. The reason might be ABA triblock copolymer show capable of forming a stereocomplex with the PLA matrix, which was used as the sole strengthening agent to modify the physical strength of PLA.^{44,45} On the other

hand, we speculated that the increase of fiber crystallinity might play an effective role in improvement of mechanical properties of PLA/PCEC hybrid scaffolds.

To validate the cell response of PLA/PCEC hybrid scaffolds, the behavior of hPMSCs cultured on the scaffolds was observed. We evaluated cells' metabolic activity and viability by MTT assay (Figure 9D), cell morphology and cell interaction with the hybrid scaffolds by fluorescent microscopic images (Figure 9A–C), and cell differential ability by SEM and alizarin red staining (Figure 10). The results revealed that hPMSCs interacted and integrated well with surrounding fibers, and could proliferate and spread well on the membranes. Moreover, after 2 weeks' incubation in osteogenic differential medium, the hPMSCs cultured on PLA/PCEC fibrous scaffolds clearly showed matrix mineralization with alizarin red staining. On the whole, the PLA/PCEC electrospun scaffolds showed good cellular compatibility and favorable osteogenic potential *in vitro*, thus should be suitable candidates for application in bone tissue engineering.

Conclusion

In this study, PLA blending with different concentrations of ABA triblock copolymer PCEC were electrospun into nano-to microfibers, with numerous nanopores on the surface of a single fiber, and they exhibited improvement of morphology and mechanical properties compared to neat PLA fiber membrane. With the ratio of PCEC increasing from 0% to 50%, average diameter of fiber and water contact angle of membrane decreased, while mechanical properties and thermal characteristics clearly improved. The biocompatibility of the scaffolds to hPMSCs was demonstrated by MTT. Favorable interactions between hPMSCs on the scaffolds were demonstrated by cell morphology, proliferation, and differentiation studies. These results definitely prove the potential of these scaffolds for bone tissue engineering. In our further research, the mechanism of triblock copolymer improving PLA mechanical properties will be studied, and this type of bone tissue substitute will be explored *in vivo*.

Acknowledgments

This work was financially supported by National Natural Sciences Foundation of China (81372446), National S&T Major Project (2011ZX09102-001-10 and 2013ZX09301304-007), and Sichuan Provincial Science and Technology Department Support Project (2011SZ0222). The authors are grateful to Wang Hui, Xie Yani, and Wen Jiqui (Analytical and Testing Center, Sichuan University) for their assistance with SEM observation, FT-IR analysis, and XRD analysis respectively.

Disclosure

The authors report no conflicts of interest in this work.

References

- de Peppo GM, Marcos-Campos I, Kahler DJ, et al. Engineering bone tissue substitutes from human induced pluripotent stem cells. *Proc Natl Acad Sci U S A*. 2013;110(21):8680–8685.
- Schubert T, Lafont S, Beaurin G, et al. Critical size bone defect reconstruction by an autologous 3D osteogenic-like tissue derived from differentiated adipose MSCs. *Biomaterials*. 2013;34(18):4428–4438.
- Salgado AJ, Coutinho OP, Reis RL. Bone tissue engineering: state of the art and future trends. *Macromol Biosci*. 2004;4(8):743–765.
- Dong SW, Ying DJ, Duan XJ, et al. Bone regeneration using an acellular extracellular matrix and bone marrow mesenchymal stem cells expressing cbfa1. *Biosci Biotechnol Biochem*. 2009;73(10):2226–2233.
- Bueno EM, Glowacki J. Cell-free and cell-based approaches for bone regeneration. *Nat Rev Rheumatol*. 2009;5(12):685–697.
- Guo G, Yu J, Luo Z, et al. Synthesis and characterization of poly(methyl methacrylate-butyl acrylate)/nano-titanium oxide composite particles. *J Nanosci Nanotechnol*. 2011;11(6):4923–4928.
- Green D, Walsh D, Mann S, Oreffo RO. The potential of biomimesis in bone tissue engineering: lessons from the design and synthesis of invertebrate skeletons. *Bone*. 2002;30(6):810–815.
- Zhang DM, Tong AP, Zhou LX, Fang F, Guo G. Osteogenic differentiation of human placenta-derived mesenchymal stem cells (PMSCs) on electrospun nanofiber meshes. *Cytotechnology*. 2012;64(6):701–710.
- Fan RR, Zhou LX, Song W, et al. Preparation and properties of g-TTCP/PBS nanocomposites and its in vitro biocompatibility assay. *Int J Biol Macromol*. 2013;59:227–234.
- Parizek M, Douglas TE, Novotna K, et al. Nanofibrous poly(lactide-co-glycolide) membranes loaded with diamond nanoparticles as promising substrates for bone tissue engineering. *Int J Nanomedicine*. 2012;7:1931–1951.
- Lutolf MP, Hubbell JA. Synthetic biomaterials as instructive extracellular microenvironments for morphogenesis in tissue engineering. *Nat Biotechnol*. 2005;23(1):47–55.
- Borjigin M, Eskridge C, Niamat R, Strouse B, Bialk P, Kmiec EB. Electrospun fiber membranes enable proliferation of genetically modified cells. *Int J Nanomedicine*. 2013;8:855–864.
- Bhattarai SR, Bhattarai N, Yi HK, Hwang PH, Cha DI, Kim HY. Novel biodegradable electrospun membrane: scaffold for tissue engineering. *Biomaterials*. 2004;25(13):2595–2602.
- Vozzi G, Flaim CJ, Bianchi F, Ahluwalia A, Bhatia S. Microfabricated PLGA scaffolds: a comparative study for application to tissue engineering. *Mater Sci Eng C Mater Biol Appl*. 2002;20(1–2):43–47.
- Tu CF, Cai Q, Yang J, Wan YQ, Bei JZ, Wang S. The fabrication and characterization of poly(lactic acid) scaffolds for tissue engineering by improved solid-liquid phase separation. *Polym Adv Technol*. 2003;14(8):565–573.
- Vasita R, Katti DS. Nanofibers and their applications in tissue engineering. *Int J Nanomedicine*. 2006;1(1):15–30.
- Liang D, Hsiao BS, Chu B. Functional electrospun nanofibrous scaffolds for biomedical applications. *Adv Drug Deliv Rev*. 2007;59(14):1392–1412.
- Abdal-hay A, Sheikh FA, Lim JK. Air jet spinning of hydroxyapatite/poly(lactic acid) hybrid nanocomposite membrane mats for bone tissue engineering. *Colloids Surf B Biointerfaces*. 2013;102:635–643.
- Rujitanaroj PO, Pimpha N, Supaphol P. Wound-dressing materials with antibacterial activity from electrospun gelatin fiber mats containing silver nanoparticles. *Polymer*. 2008;49(21):4723–4732.
- Guo G, Fu SZ, Zhou LX. Preparation of curcumin loaded poly(ϵ -caprolactone)-poly(ethylene glycol)-poly(ϵ -caprolactone) nanofibers and their in vitro antitumor activity against glioma 9L cells. *Nanoscale*. 2011;3(9):3825–3832.
- Alhosseini SN, Moztaaradeh F, Mozafari M, et al. Synthesis and characterization of electrospun polyvinyl alcohol nanofibrous scaffolds modified by blending with chitosan for neural tissue engineering. *Int J Nanomedicine*. 2012;7:25–34.
- Bognitzki M, Czado W, Frese T, et al. Nanostructured fibers via electrospinning. *Adv Mater*. 2001;13(1):70–72.
- Somvipart S, Kanokpanont S, Rangkupan R, Ratanavaraporn J, Damrongsakkul S. Development of electrospun beaded fibers from Thai silk fibroin and gelatin for controlled release application. *Int J Biol Macromol*. 2013;55:176–184.
- Pelto J, Björninen M, Pälli A, et al. Novel polypyrrole-coated polylactide scaffolds enhance adipose stem cell proliferation and early osteogenic differentiation. *Tissue Eng Part A*. 2013;19(7–8):882–892.
- Boland ED, Telemeco TA, Simpson DG, Wnek GE, Bowlin GL. Utilizing acid pretreatment and electrospinning to improve biocompatibility of poly(glycolic acid) for tissue engineering. *J Biomed Mater Res Part B Appl Biomater*. 2004;71(1):144–152.
- Zhang CL, Lv KP, Cong HP, Yu SH. Controlled assemblies of gold nanorods in PVA nanofiber matrix as flexible free-standing SERS substrates by electrospinning. *Small*. 2012;8(5):648–653.
- Fan RR, Zhou LX, Li DX, Zhang DM, Wu M, Guo G. Preparation and characterization of composites based on poly (butylene succinate) and poly (lactic acid) grafted tetracalcium phosphate. *Journal of Macromolecular Science, Part B: Physics*. Epub July 29, 2013.
- Rathi S, Coughlin EB, Hsu SL, Golub CS, Ling GH, Tzivianis MJ. Effect of midblock on the morphology and properties of blends of ABA triblock copolymers of PDLA-mid-block-PDLA with PLLA. *Polymer*. 2011;53(14):3008–3016.
- Chiou BS, Jafri H, Avena-Bustillos R, et al. Properties of electrospun pollock gelatin/poly(vinyl alcohol) and pollock gelatin/poly(lactic acid) fibers. *Int J Biol Macromol*. 2013;55:214–220.
- Chen CC, Chueh JY, Tseng H, Huang HM, Lee SY. Preparation and characterization of biodegradable PLA polymeric blends. *Biomaterials*. 2003;24(7):1167–1173.
- Chen HL, Huang J, Yu JH, Liu SY, Gu P. Electrospun chitosan-graft-poly(ϵ -caprolactone)/poly(ϵ -caprolactone) cationic nanofibrous mats as potential scaffolds for skin tissue engineering. *Int J Biol Macromol*. 2010;48(1):13–19.
- Chen GX, Kim HS, Kim ES, Yoon JS. Compatibilization-like effect of reactive organoclay on the poly(L-lactide)/poly(butylene succinate) blends. *Polymer*. 2005;46(25):11829–11836.
- Hu Y, Hu YS, Topolkaev V, Hiltner A, Baer E. Aging of poly(lactide)/poly(ethylene glycol) blends. Part 2. Poly(lactide) with high stereoregularity. *Polymer*. 2003;44(19):5711–5720.
- Horwitz EM, Le Blanc K, Dominici M, et al. Clarification of the nomenclature for MSC: The International Society For Cellular Therapy position statement. *Cytotherapy*. 2005;7(5):393–395.
- Hosseinkhani H, Hong PD, Yu DS, et al. Development of 3D in vitro platform technology to engineer mesenchymal stem cells. *Int J Nanomedicine*. 2012;7:3035–3043.
- Uccelli A, Moretta L, Pistoia V. Mesenchymal stem cells in health and disease. *Nat Rev Immunol*. 2008;8(9):726–736.
- Brooke G, Rossetti T, Pelekanos R, et al. Manufacturing of human placenta-derived mesenchymal stem cells for clinical trials. *Br J Haematol*. 2009;144(4):571–579.
- Bartholomew A, Sturgen C, Siatskas M et al. Mesenchymal stem cells suppress lymphocyte proliferation in vitro and prolong skin graft survival in vivo. *Exp Hematol*. 2002;30(1):42–48.
- Soleimani M, Nadri S. A protocol for isolation and culture of mesenchymal stem cells from mouse bone marrow. *Nat Protoc*. 2009;4(1):102–106.
- Matikainen T, Laine J. Placenta – an alternative source of stem cells. *Toxicol Appl Pharmacol*. 2005;207(Suppl 2):544–549.
- Nazarov I, Lee JW, Soupene E, et al. Multipotent stromal stem cells from human placenta demonstrate high therapeutic potential. *Stem Cells Transl Med*. 2012;1(5):359–372.

42. Portmann-Lanz CB, Schoebedein A, Huber A, et al. Placental mesenchymal stem cells as potential autologous graft for pre- and perinatal neuroregeneration. *Am J Obstet Gynecol.* 2006;194(3):664–673.
43. In 't Anker PS, Scherjon SA, Kleijburg-van der Keur C, et al. Isolation of mesenchymal stem cells of fetal or maternal origin from human placenta. *Stem Cells.* 2004;22(7):1338–1345.
44. Yang JJ, Liang YR, Luo J, Zhao CZ, Han CC. Multilength scale studies of the confined crystallization in poly(L-lactide)-block-poly(ethylene glycol) copolymer. *Macromolecules.* 2012;45(10):4254–4261.
45. Hébert JS, Wood-Adams P, Heuzey MC, Dubois C, Brisson J. Morphology of polylactic acid crystallized during annealing after uniaxial deformation. *J Polym Sci B Polym Phys.* 2013;51(6):430–440.

International Journal of Nanomedicine

Dovepress

Publish your work in this journal

The International Journal of Nanomedicine is an international, peer-reviewed journal focusing on the application of nanotechnology in diagnostics, therapeutics, and drug delivery systems throughout the biomedical field. This journal is indexed on PubMed Central, MedLine, CAS, SciSearch®, Current Contents®/Clinical Medicine,

Journal Citation Reports/Science Edition, EMBase, Scopus and the Elsevier Bibliographic databases. The manuscript management system is completely online and includes a very quick and fair peer-review system, which is all easy to use. Visit <http://www.dovepress.com/testimonials.php> to read real quotes from published authors.

Submit your manuscript here: <http://www.dovepress.com/international-journal-of-nanomedicine-journal>